

Detection and Recognition: A Pairwise Interaction Framework for Mobile Service Robots

Mengyu Liang, Sarah Gillet Schlegel, Iolanda Leite

Abstract—Autonomous mobile service robots, like lawnmowers or cleaning robots, operating in human-populated environments need to reason about local human-human interactions to support safe and socially aware navigation while fulfilling their tasks. For such robots, interaction understanding is not primarily a fine-grained recognition problem, but a perception problem under limited sensing quality and computational resources. Many existing approaches focus on holistic group activity recognition, which often requires complex and large models which may not be necessary for mobile service robots. Others use pairwise interaction methods which commonly rely on skeletal representations but their use in outdoor environments remains challenging. In this work, we argue that pairwise human interaction constitute a minimal yet sufficient perceptual unit for robot-centric social understanding. We study the problem of identifying interacting person pairs and classifying coarse-grained interaction behaviors sufficient for downstream group-level reasoning and service robot decision-making. To this end, we adopt a two-stage framework in which candidate interacting pairs are first identified based on lightweight geometric and motion cues, and interaction types are subsequently classified using a relation network. We evaluate the proposed approach on the JRDB dataset, where it achieves sufficient accuracy with reduced computational cost and model size compared to appearance-based methods. Additional experiments on the Collective Activity Dataset (CAD) and zero shot test on a lawnmower-collected dataset further illustrate the generality of the proposed framework. These results suggest that pairwise geometric and motion cues provide a practical and efficient basis for interaction-aware perception on mobile service robot providing a promising method for integration into mobile robot navigation stacks in future work.

I. INTRODUCTION

Autonomous mobile robots operating in human-populated environments must continuously reason about nearby people to navigate safely and make appropriate decisions [16, 3, 27]. For outdoor platforms such as delivery robots or lawnmowers, the primary requirement is not fine-grained action recognition, but a robust and coarse understanding of how nearby people are socially organized, for example, whether individuals are walking together, standing in a group, or sitting nearby. Such interaction-level understanding provides actionable constraints for collision avoidance, path planning, and behavior modulation, while remaining compatible with the limited sensing quality and computational resources available on mobile robot.

Group activity recognition (GAR) has been extensively studied due to its applications in surveillance, sports analysis, social scene understanding, and elderly care [5, 29, 4]. Most GAR methods adopt a holistic formulation that treats the scene as a single unit and predicts a dominant group-level activity [28]. While effective in offline analysis, such formulations provide limited guidance for socially appropriate

robot behavior. For example, when navigating through a public space, a robot may need to distinguish between walking individuals and multiple small sitting groups in order to choose a socially acceptable path. From a robot’s perspective, only a subset of individuals are relevant but multiple interactions may happen within the same scene [16]. In crowded outdoor environments, accurately identifying whether individuals are interacting is more important than recognizing a single global group activity. Rather than replacing group activity recognition, we view pairwise interaction modeling of two persons as a more actionable intermediate representation for robot, which can be flexibly aggregated into group-level reasoning when needed.

Pairwise human-human interaction (HHI) recognition, which we refer to simply as pairwise interaction in the remainder of this paper, explicitly models relations between two individuals and therefore offers potential to capture localized social interactions in complex and crowded scenes [17, 22, 19]. Existing pairwise approaches often rely on skeleton-based features [16], which are fragile in outdoor scenarios due to occlusion, clutter, and low-resolution imagery, and often require computationally expensive processing pipelines [11]. These assumptions fundamentally conflict with the sensing conditions and real-time constraints of outdoor mobile robots.

In this work, we formulate pairwise interaction recognition as a perceptual task for mobile robots. We argue that pairwise interactions represent the smallest social unit that still imposes meaningful information on robotic navigation and decision-making. We adopt a robot centered two-stage framework that separates interaction detection and interaction classification. In the first stage, candidate interacting pairs are identified using low-dimensional geometric cues derived from person bounding boxes. In the second stage, only these candidate pairs are classified into coarse-grained interaction types, e.g., walking, standing, or sitting together, by combining motion cues from optical flow with relational reasoning.

By relying exclusively on bounding box geometry and optical flow, both of which are robustly available from modern perception stacks in outdoor environments, our approach avoids skeleton extraction and heavy visual backbones. This design reflects a deliberate choice to favor minimal and sufficient interaction recognition over increasingly complex models, making the proposed framework well suited for deployment on resource-constrained mobile robot platforms.

To summarize, our contributions are listed as follows:

- We introduce a robot centered formulation of human-human interaction recognition that focuses on detecting

interacting pairs and coarse-grained interaction types, tailored to mobile service robotic applications.

- We propose an efficient two-stage pipeline that performs interaction detection and classification using bounding boxes and optical flow, avoiding reliance on skeleton-based representations.
- Through extensive ablation studies, we provide evidence that geometry and motion cues dominate performance for coarse-grained interaction classification, while complex appearance features offer limited additional benefit.
- We evaluate our approach on the JRDB dataset and Collective Activity datasets, and demonstrate robust zero shot transfer to a mobile lawnmower platform, highlighting the practicality of the proposed interaction recognition method under real-world robotic conditions.

II. RELATED WORK

A. Group Activity Recognition

Group activity recognition (GAR) has been extensively studied in computer vision for understanding collective behaviors in surveillance and social scene analysis [4]. Early approaches [14, 10, 2] relied on handcrafted features and spatio-temporal relationships among individuals, while more recent methods employ deep neural networks and graph-based formulations to model interactions implicitly across all people in a scene [25, 28, 30]. Despite their success in predicting scene-level activity labels, most GAR methods adopt a holistic formulation, treating the entire scene as a single unit and inferring a dominant group activity. Such formulations are not well suited with robotic perception needs, as multiple local interactions may occur simultaneously in the robot’s view. From those interactions, only a subset of nearby individuals is relevant for navigation and decision-making.

B. Pairwise Interaction Recognition

Pairwise interaction recognition explicitly models the relationship between two individuals [16]. By focusing on localized interactions, pairwise approaches are better suited to scenarios where multiple interactions coexist and explicit interaction localization is required [22, 19].

1) *Skeleton-based Approaches*: Skeleton-based representations have been widely adopted for pairwise interaction recognition due to their ability to explicitly encode human pose and joint-level relationships. Graph-based models, such as two-person GCNs [16], have demonstrated strong performance on benchmark datasets under controlled conditions [20, 17]. However, skeleton-based methods rely heavily on accurate pose estimation, which is often unreliable in crowded or outdoor environments due to occlusion, motion blur, and low-resolution imagery [16]. In addition, pose extraction and graph-based processing introduce substantial computational cost. These limitations make skeleton-based interaction recognition less suitable for real-time perception on mobile robots operating under sensing and resource constraints.

2) *Appearance- and Relation-based Approaches*: To reduce dependence on pose quality, several works incorporate RGB appearance features into relational reasoning frameworks. Interaction relational networks [20] and attention-augmented relation models [1] combine visual features with relational modules to infer interactions between individuals, while non-local architectures [26] generalize relational reasoning to arbitrary region pairs. Although effective in controlled settings, such appearance approaches typically require deep visual backbones and high capacity relation modules, resulting in significant computational cost. For coarse-grained interaction recognition in robotic scenarios, such modeling method is often heavy to compute, especially when motion and spatial cues already provide strong discriminative signals. This raises questions about the accuracy–efficiency trade-off of appearance centered interaction models for robotic deployment.

3) *Geometry- and Motion-based Interaction Modeling*: Prior to the dominance of pose- and appearance-based methods, early work on interaction recognition explored handcrafted geometric and motion cues [28, 29, 15, 21], such as relative distance, spatial overlap, and motion correlation between individuals. These approaches demonstrated that interaction patterns can be inferred from simple spatial and temporal relationships, with minimal computational requirements. Our work revisits geometric and motion cues from a robot centered perspective as the core representation within a interaction detection and classification pipeline. By systematically integrating bounding box geometry and optical flow into a two-stage framework, we aim to retain the efficiency and robustness of cues while enabling explicit and pairwise interaction reasoning.

III. METHOD

In this paper, we use interaction detection to refer to identifying whether a pair of individuals is interacting, interaction classification to denote categorizing the interaction type, and interaction recognition to describe the overall perception task combining both stages.

We adopt a two-stage framework for social interaction recognition, designed to balance interaction modeling capability with computational efficiency for mobile service robot.

Stage 1 performs **pairwise interaction detection** as illustrated in Fig 1. We use geometric cues derived from people’s bounding boxes to identify whether two individuals are socially interacting. This stage estimates whether two individuals are likely to be socially interacting. Rather than aiming for optimal interaction classification, Stage 1 serves as a high recall interaction proposal mechanism that filters out clearly non-interacting pairs for further analysis.

Stage 2 operates on the interaction proposals generated by Stage 1 and performs **coarse-grained interaction classification**. By restricting classification to a set of candidate interacting pairs, this stage integrates geometric and motion cues with frozen visual appearance features to refine interaction understanding while maintaining computational efficiency.

The overall architecture has the following components:

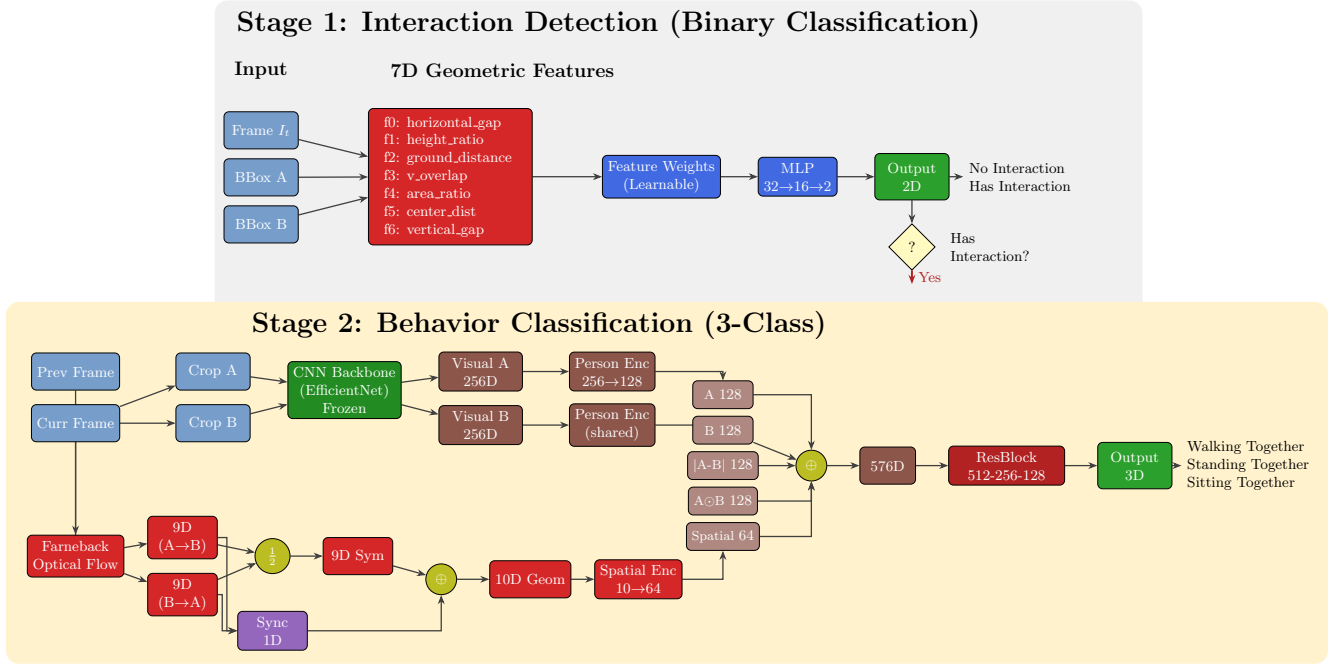


Fig. 1: **Overview of the proposed two-stage pairwise interaction recognition framework:** **Stage 1** performs interaction detection using a 7D geometric feature vector derived from bounding box configurations, producing candidate interacting person pairs. **Stage 2** classifies coarse-grained interaction types by combining frozen visual appearance features extracted by EfficientNet with geometric–motion features computed from optical flow, using a relation network for explicit pairwise reasoning. The framework is designed for efficient and robust deployment on constrained resource robotic platforms.

- **Geometric Interaction Module (Stage 1):** A classifier that infers pairwise interaction likelihoods from low-dimensional geometric features.
- **Frozen EfficientNet Backbone:** A pretrained EfficientNet [24] used for appearance feature extraction and kept frozen throughout training.
- **Geometric Flow Extractor:** A Farneback module [7] that computes motion features between interacting persons.
- **Relation Network (Stage 2):** A trainable classification head that performs explicit relational reasoning over interacting person pairs.

The system predicts coarse-grained interaction categories that can be distinguished by motion or global pose changes sufficient for downstream robotic navigation and decision-making. In this work, we focus on *Walking Together*, *Standing Together*, and *Sitting Together*.

A. Feature Extraction Pipeline

1) *Stage 1: Pairwise Interaction Detection:* Given detected person pairs within a frame, Stage 1 formulates interaction detection as a binary classification task. For each pair, we extract a 7D geometric feature vector from the corresponding bounding boxes, encoding relative distance, scale, overlap, and vertical alignment. These features provide a description of spatial relationships commonly associated with social interaction

[25].

To account for the varying importance of different geometric cues, we apply a learnable feature reweighting transformation $T(\mathbf{g})$, followed by a shallow classifier C to estimate pairwise interaction likelihoods:

$$T(\mathbf{g}) = (\mathbf{g} + \mathbf{b}) \odot \mathbf{s} \odot \mathbf{w} \quad (1)$$

where $\mathbf{g} \in \mathbb{R}^{d_g}$ is the input geometric feature vector, $\mathbf{b} \in \mathbb{R}^{d_g}$ and $\mathbf{s} \in \mathbb{R}^{d_g}$ are learnable vectors and $\mathbf{w} \in \mathbb{R}^{d_g}$ is learnable weights. \mathbf{s} and \mathbf{w} are initialized to one, while \mathbf{b} is initialized to zero to obtain a stable start.

We form classifier C as

$$C = \text{Linear}(d_g \rightarrow h_1) \rightarrow \text{ReLU} \rightarrow \text{Dropout}(p) \rightarrow \text{Linear}(h_1 \rightarrow h_2) \rightarrow \text{ReLU} \rightarrow \text{Dropout}(p) \rightarrow \text{Linear}(h_2 \rightarrow 2) \quad (2)$$

with default configuration $h_1 = 32$, $h_2 = 16$, and dropout rate $p = 0.1$.

This design enables the model to adaptively emphasize informative geometric relationships while maintaining low computational cost.

At inference time, pairwise predictions can be clustered into an interaction graph where connected components represent candidate social groups for evaluation. This stage is designed to prioritize recall over precision by limiting negative samples

and using lower threshold θ , reflecting the asymmetry of risk in robotic interaction perception: missing an interaction may have greater consequences for navigation and safety than temporarily considering a negative interaction. The results are passed to Stage 2 for further classification.

2) *Stage 2: Appearance and Motion Features*: For each interacting person pair p_i identified in Stage 1, Stage 2 extracts both appearance and motion cues before classifying coarse-grained interaction categories.

We obtain appearance features using a frozen EfficientNet [24] backbone applied to cropped person regions. We opted for freezing the backbone to improve data efficiency and prevent overfitting on the limited interaction data we had available.

We extract optical flow field using dense optical flow computed between consecutive frames through the Farneback [7] method. From the optical flow field and bounding box geometry, we encode relative distance, bounding box configuration, motion magnitude statistics, and motion consistency between two persons to compute a $10D$ geometric(f_1 to f_5)-motion(f_6 to f_{10}) feature. With (x, y, w, h) as the bounding box of person A or B , H_{img} and W_{img} as image height and width, $\mathbf{F} \in \mathbb{R}^{H_{\text{img}} \times W_{\text{img}} \times 2}$ as the Dense optical flow field and M the valid optical flow area where $\mathbf{F}_x = \mathbf{F}_{::,0}$ and $\mathbf{F}_y = \mathbf{F}_{::,1}$ define the horizontal and vertical flow components (positive = rightward and downward), we define the features as follows:

$$f_1 = \frac{d_{AB}}{h}, \quad f_2 = \frac{d_{AB}}{\bar{w}} \quad (3)$$

$$r_A = \frac{h_A}{w_A}, r_B = \frac{h_B}{w_B} \quad f_3 = \frac{r_A + r_B}{2} \quad (4)$$

$$\text{bottom}_A = y_A + h_A, \quad \text{bottom}_B = y_B + h_B, \\ f_4 = \frac{\bar{h}}{H_{\text{img}}}, \quad f_5 = \frac{\frac{\text{bottom}_A + \text{bottom}_B}{2}}{H_{\text{img}}} \quad (5)$$

$$\mathbf{E} = \sqrt{(|\mathbf{F}_x|)^2 + (\mathbf{F}_y)^2}, \quad \bar{a} = \frac{w_A h_A + w_B h_B}{2} \\ f_6 = \frac{\mu(\mathbf{E})}{\bar{a}}, \quad f_7 = \frac{\sigma(\mathbf{E})}{\bar{a}} \quad (6)$$

$$\bar{v} = \mu(|\mathbf{F}_y|), \quad \bar{h} = \mu(|\mathbf{F}_x|), \quad f_8 = \frac{\bar{v}}{\max(\bar{h}, \epsilon)} \quad (7)$$

$$\mathbf{V} = \sqrt{\mathbf{F}_x^2 + \mathbf{F}_y^2}, \quad \Theta = \arctan 2(\mathbf{F}_y, \mathbf{F}_x) \\ \bar{C} = \frac{\sum \cos(\Theta) \odot \mathbf{M}}{\sum \mathbf{M}}, \quad \bar{S} = \frac{\sum \sin(\Theta) \odot \mathbf{M}}{\sum \mathbf{M}} \\ f_9 = \sqrt{\bar{C}^2 + \bar{S}^2} \quad (8)$$

To quantify motion coordination between two people, we compute an interaction synchrony feature (f_{10}) that aggregates 4 similarity measures calculated from f_3, f_6, f_7, f_8 , including flow magnitude similarity, temporal motion pattern similarity, posture consistency, and dominant motion direction alignment. The final geometric-motion feature vector is defined as:

$$\mathbf{g} = [f_1, f_2, \dots, f_{10}]^T \in \mathbb{R}^{10}. \quad (9)$$

To ensure permutation invariance with respect to person ordering, asymmetric features are computed from both $A \rightarrow B$ and $B \rightarrow A$ perspectives and symmetrized by averaging.

B. Stage 2: Relation Network Classifier

Stage 2 performs interaction classification using a relation network that explicitly models pairwise relationships. We project each person's appearance feature v_A, v_B using a shared encoder

$$\mathbf{e}_A = \text{PersonEnc}(v_A), \quad \mathbf{e}_B = \text{PersonEnc}(v_B) \quad (10)$$

where PersonEnc is a shared two layer MLP with BatchNorm and SiLU activations.

The interaction representation is then constructed by combining the two person appearance feature with their encoded geometric-motion features f using concatenation operations. Then the resulting interaction feature is passed to a MLP classifier to predict the interaction category.

$$R = \text{Concat}(\mathbf{e}_A, \mathbf{e}_B, |\mathbf{e}_A - \mathbf{e}_B|, \mathbf{e}_A \odot \mathbf{e}_B, \mathbf{s}) \rightarrow \\ \text{Linear}(1152 \rightarrow 512) \rightarrow \text{BN} \rightarrow \text{SiLU} \rightarrow \text{Dropout}(p) + \text{Res} \rightarrow \\ \text{Linear}(512 \rightarrow 256) \rightarrow \text{BN} \rightarrow \text{SiLU} \rightarrow \text{Dropout}(p) + \text{Res} \rightarrow \\ \text{Linear}(256 \rightarrow 128) \rightarrow \text{BN} \rightarrow \text{SiLU} \rightarrow \text{Dropout}(p) + \text{Res} \rightarrow \\ \text{Linear}(128 \rightarrow 3) \quad (11)$$

IV. EXPERIMENT

We evaluate the proposed pairwise interaction method in terms of recognition performance, computational efficiency, and robustness across datasets and deployment scenarios relevant to mobile service robots.

A. Dataset

We evaluate our approach on two public benchmarks and one custom collected dataset. The public benchmarks provide annotations for human interactions and collective activities. Our dataset follows the same annotation scheme.

JRDB [12] is a dataset designed for human social understanding in human interactions across diverse indoor and outdoor social environments like cafeteria, teaching buildings and squares. By capturing videos of people in diverse environments, this dataset intends to offer an insight into human behavior within varied social contexts. For each video frame, the dataset provides annotations at three discernible levels: individual attributes, e.g., gender and age, intra-group interactions, e.g., standing and sitting together, and social group context, e.g., sitting together in cafeteria, making it well suited for evaluating pairwise interaction detection.

In this work, we only use the annotations for intra-group context. Further, we will focus on three categories: *walking, standing and sitting together*. The reasons for only using these three categories are twofold: (1) these categories appear important for mobile robot social navigation (2) when inspecting the distribution of labels we found strong label dependencies.

For example, *conversation* frequently co-occurs with varying other behaviors, while *eating together* only appears with *conversation* and *sitting together*. This indicates that additional labels are not independent modes but variations of the chosen three dominant categories. Therefore, reducing the label space to these three classes captures a majority of the dataset’s essential structure which enables more robust modeling. We leave remaining labels and the evaluation of their importance for mobile robot navigation for future exploration. For the interested reader, we provide the label distribution and their conditional probabilities in the Appendix.

We additionally evaluate our framework on the Collective Activity Dataset (CAD) [5], which contains videos of indoor and outdoor scenes with annotated group activities. Following prior work [6], we use the annotated social activity labels for training and evaluation.

We also collected data using a forward-facing, low-angle camera mounted on the lawnmower at 6 scenes on a university campus, resulting in 14 minutes video streams with a resolution of 648×486 at 15 fps. The data is annotated with about 2k interactions in total for a zero shot evaluation.

B. Data Filtering and Preprocessing

We apply filtering to improve data reliability and remove false positive bounding boxes. We remove heavily occluded individuals and discard detections close to image boundaries, which were often incomplete, unstable or empty, i.e., did not resemble a person. Frames are sampled at an interval to reduce temporal redundancy while preserving interaction consistency.

During training, random horizontal flipping is applied for data augmentation. Class imbalance is handled through weighted sampling combined with a focal loss.

C. Implementation Details

We use EfficientNet [24] as the default visual backbone due to its performance, and kept it frozen throughout training. To analyze the impact of appearance features, we additionally evaluate ResNet [8], VGG [23], AlexNet [13], and MobileNet [9] under the same training protocol.

The model is trained using AdamW [18] with a fixed learning rate of 1×10^{-4} and weight decay of 1×10^{-5} .

D. Evaluation Metrics

We report Accuracy, Mean Per-Class Accuracy (MPCA), and Macro F1-score to account for class imbalance:

$$\text{Accuracy} = \frac{\sum_{i=1}^N [\hat{y}_i = y_i]}{N} \quad (12)$$

$$\text{MPCA} = \frac{1}{C} \sum_{c=1}^C \frac{TP_c}{N_c} = \frac{1}{C} \sum_{c=1}^C \text{Recall}_c \quad (13)$$

$$\text{Macro-F1} = \frac{1}{C} \sum_{c=1}^C \frac{2 \cdot P_c \cdot R_c}{P_c + R_c} \quad (14)$$

where $P_c = TP_c / (TP_c + FP_c)$ and $R_c = TP_c / (TP_c + FN_c)$ are per-class precision and recall, respectively.

Computational efficiency is evaluated using FLOPs, particularly relevant for resource constrained robotic deployment.

E. Ablation Study

We conducted an ablation study to evaluate the contribution of appearance, motion, and geometric cues in the JRDB dataset. Results are presented in Table I.

The results show that motion and geometric features dominate performance, achieving the best overall accuracy of 84.3% without using a pretrained visual backbone. Motion features seem to have the strongest influence with a sole performance of 78.4% accuracy. Geometry features reached a sole accuracy of 59.3%, indicating that spatial proximity alone is insufficient for reliable interaction recognition.

Incorporating visual appearance features does not seem to improve accuracy and often leads to degradation, suggesting redundancy with motion and geometric cues. EfficientNet yields slightly improved class balanced performance, but without clear gains in overall accuracy. This suggests improved class balance rather than stronger discriminative power. From an efficiency perspective, removing visual backbones significantly reduces computational cost, confirming a favorable accuracy–efficiency trade-off for robotic perception.

F. Comparison to Baselines

We compare our approach with state-of-the-art methods on CAD. Existing methods are primarily designed for group detection and group level activity recognition, whereas our approach focuses on pairwise interaction detection. The results are captured in Table II.

To enable fair comparison, we map pairwise interaction predictions to group structures by connecting interacting individuals, and determine group activities via majority voting over predicted interaction types.

On the CAD dataset, our approach (79.8%, 52.6%) consistently outperforms naive baselines that assume a single group (54.4%, 51.6%) or no grouping (62.4%, 54.9%) in grouping, reinforcing prior findings that highlight the importance of modeling group membership. Compared to unsupervised clustering methods (78.2%, 52.2%), our approach achieves comparable or improved grouping accuracy while maintaining lower model complexity. Although fully supervised grouping methods (83.0%, 69.0%) achieve higher accuracy, they require larger models and stronger supervision, making them less suitable for real-time robotic deployment.

G. Zero Shot Inference on Lawnmower Dataset

We further evaluate our approach through zero-shot deployment on a mobile lawnmower platform operating in an outdoor environment, using the model trained on JRDB without any additional fine-tuning or retraining. Examples images and their annotations are shown in Figure 2.

Despite the domain shift in camera viewpoint, platform motion, and scene dynamics, our interaction detection stage achieves a precision of 96.5%, successfully identifying the majority of interacting person pairs. Missed detections are

appearance	motion	geometric	Acc/%	MPCA/%	Macro F1	flops
/	/	y	59.3 ± 3.1	66.1 ± 2.0	0.644 ± 0.020	1.08Mb
/	y	/	78.4 ± 0.3	56.5 ± 0.0	0.554 ± 0.002	1.08Mb
/	y	y	84.3 ± 1.8	79.6 ± 0.9	0.772 ± 0.008	1.12Mb
efficientnet_v2_s	y	y	80.0 ± 2.6	80.3 ± 1.1	0.765 ± 0.012	5.80Gb
efficientnet_v2_s	/	y	78.7 ± 2.4	78.4 ± 1.8	0.774 ± 0.015	5.80Gb
efficientnet_v2_s	y	/	74.6 ± 3.5	70.8 ± 2.3	0.710 ± 0.015	5.80Gb
efficientnet_v2_s	/	/	77.1 ± 3.0	69.6 ± 1.5	0.711 ± 0.012	5.80Gb
mobilenet_v3_s	y	y	75.5	72.8	0.727	122.51Mb
resnet18	y	y	74.8	76.3	0.765	975.16Mb
vgg16	y	y	74.8	74.6	0.724	7.68Gb
alexnet	y	y	75.0	77.2	0.710	292.26Mb

TABLE I: Ablation study of visual, motion, and geometric cues on JRDB with Accuracy (Acc), Mean Per-Class Accuracy (MPCA), Macro F1-score, and computational cost (FLOPs). Result with \pm are tested with three random seed: 42,59,108. The results show that motion and geometric cues dominate performance, achieving the highest accuracy without relying on a visual backbone. Incorporating appearance features provides limited or negative gains while increasing computational cost, highlighting a favorable accuracy–efficiency trade-off for geometry and motion features in robotic perception.

	Membership	Social Activity
	Acc.%	Acc.%
ARG [28][group]	54.4	47.2
I3D-SA-GAT [6][group]	54.4	47.7
GT[group]	54.4	51.6
ARG [28][individuals]	62.4	49.0
I3D-SA-GAT [6][individuals]	62.4	49.5
GT[individuals]	62.4	54.9
I3D-SA-GAT [6][cluster]	78.2	52.2
I3D-SA-GAT [6][learn2cluster]	83.0	69.0
ours	79.8	52.6

TABLE II: Comparison with state-of-the-art methods on the Collective Activity Dataset (CAD): Our pairwise interaction based approach is evaluated under both group-level and individual-level settings by mapping predicted interactions to group structures. The results demonstrate that explicit modeling of pairwise interactions outperforms naive grouping baselines and achieves competitive performance compared to more complex clustering based and fully supervised methods, while maintaining lower model complexity.

primarily caused by low image resolution and partial visibility of distant pedestrians. The overall processing speed offline reaches 44 frames per second exceeding the camera capturing speed of 15 fps, demonstrating the suitability of the proposed pipeline for real-time deployment on mobile robotic platforms.

For interaction type recognition, the stage 2 classifier achieves a macro F1-score of 0.51. Notably, the recall for the walking together and standing together classes reaches 98.5% and 100%, respectively, indicating strong robustness for common interaction patterns encountered during navigation. Most classification errors occur when sitting together interactions are misclassified as walking together. This behavior can be attributed to platform induced motion: although motion compensation is applied during optical flow computation, the rapidly changing visual content caused by lawnmower movement, including periodic wobbling due to irregularities in the grass surface, and low camera angle sometimes occluded by grass introduces flow patterns that are difficult to distinguish

from human motion. Since the model is trained on data collected from static cameras, this represents a challenging zero shot transfer scenario.

V. DISCUSSION

This work explores pairwise human interaction detection as a fundamental perceptual unit for robotic systems operating in outdoor environments. By explicitly focusing on local interactions rather than holistic group activity recognition and coarse-grained interaction categories, our approach emphasizes capturing what is most relevant for mobile robots, which typically require nearby and actionable social cues under limited sensing and computational resources.

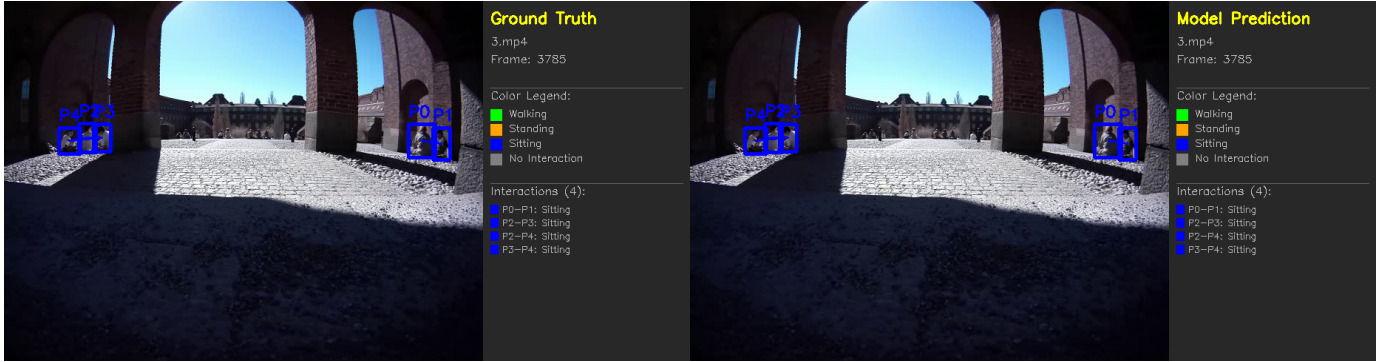
A key design choice of our method is the reliance on bounding box geometry and motion cues, avoiding skeletal representations and heavy visual backbones. The experimental results suggest that these lightweight cues are sufficient to capture essential interaction patterns for coarse-grained social activity recognition with similar performance or acceptable loss in accuracy. At the same time, the lightweight nature of our approach offers advantages in computational efficiency and robustness. The ablation and baseline comparisons further indicate that motion and positional cues dominate performance, whereas increasingly complex visual features often yield diminishing returns. With these findings, we want to highlight that detailed appearance or pose information might not always be necessary for effective social activity recognition. We would like to encourage the community to complement the push for large models with the exploration of lightweight and simple approaches particularly when concerned with outdoor or resource constrained robotic settings.

A. Limitations

At the same time, the proposed approach has limitations. The coarse activity categories considered in this work may not capture more subtle or long-term social behaviors. In addition, the current framework assumes reliable person detection and tracking, and its performance may degrade under severe occlusions or crowded scenes. Future work should further



(a)



(b)



(c)

Fig. 2: **Qualitative zero shot interaction recognition results on data collected from a mobile lawnmower platform** (a) The lawnmower moves rapidly through a group of pedestrians, inducing strong ego-motion and viewpoint changes, which lead to misclassifications of interaction types. (b) The lawnmower remains stationary, resulting in stable observations and correct interaction recognition most person pairs. (c) The lawnmower approaches two individuals engaged in a face-to-face interaction, illustrating the intended use case of interaction aware perception to support downstream robotic decision-making.

explore the suitability of this approach in varying scenarios and integrated into a navigating social robot.

VI. CONCLUSION AND FUTURE WORK

This work presents pairwise interaction detection as a lightweight method for mobile service robots. By relying on simple geometric and motion cues, the proposed approach captures interaction information that should be sufficient for socially-aware navigation, while avoiding the computational cost of complex visual or pose-based models. These results suggest that appropriate representation choices, rather than

increased model complexity, are practical to interaction perception on resource-constrained robotic platforms.

Future work may extend this framework by incorporating longer-term temporal reasoning, selectively integrating group context when necessary, or coupling interaction perception more tightly with downstream robotic planning and control. Nonetheless, this study demonstrates that pairwise geometric and motion reasoning provides a strong and efficient foundation for interaction perception, offering a practical compromise between accuracy, interpretability, and computational cost for real-world mobile robotic systems.

REFERENCES

- [1] Farzaneh Askari, Cyril Yared, Rohit Ramaprasad, Devin Garg, Anjun Hu, and James J. Clark. Video interaction recognition using an attention augmented relational network and skeleton data. In *2024 IEEE/CVF Conference on Computer Vision and Pattern Recognition Workshops (CVPRW)*, pages 3225–3234, June 2024. doi: 10.1109/CVPRW63382.2024.00328.
- [2] Timur Bagautdinov, Alexandre Alahi, François Fleuret, Pascal Fua, and Silvio Savarese. Social scene understanding: End-to-end multi-person action localization and collective activity recognition. In *2017 IEEE Conference on Computer Vision and Pattern Recognition (CVPR)*, pages 3425–3434, July 2017. doi: 10.1109/CVPR.2017.365.
- [3] Mounir Bendali-Braham, Jonathan Weber, Germain Forestier, Lhassane Idoumghar, and Pierre-Alain Muller. Recent trends in crowd analysis: A review. *Machine Learning with Applications*, 4:100023, 2021. ISSN 2666-8270. doi: <https://doi.org/10.1016/j.mlwa.2021.100023>. URL <https://www.sciencedirect.com/science/article/pii/S2666827021000049>.
- [4] Wongun Choi, Khuram Shahid, and Silvio Savarese. What are they doing? : Collective activity classification using spatio-temporal relationship among people. In *2009 IEEE 12th International Conference on Computer Vision Workshops, ICCV Workshops*, pages 1282–1289, Sep. 2009. doi: 10.1109/ICCVW.2009.5457461.
- [5] Wongun Choi, Khuram Shahid, and Silvio Savarese. Learning context for collective activity recognition. In *CVPR 2011*, pages 3273–3280, June 2011. doi: 10.1109/CVPR.2011.5995707.
- [6] Mahsa Ehsanpour, Alireza Abedin, Fatemeh Saleh, Javen Shi, Ian Reid, and Hamid Rezaatofghi. Joint learning of social groups, individuals action and sub-group activities in videos, 2020. URL <https://arxiv.org/abs/2007.02632>.
- [7] Gunnar Farneback. Two-frame motion estimation based on polynomial expansion. volume 2749, pages 363–370, 06 2003. ISBN 978-3-540-40601-3. doi: 10.1007/3-540-45103-X_50.
- [8] Kaiming He, Xiangyu Zhang, Shaoqing Ren, and Jian Sun. Deep residual learning for image recognition, 2015. URL <https://arxiv.org/abs/1512.03385>.
- [9] Andrew G. Howard, Menglong Zhu, Bo Chen, Dmitry Kalenichenko, Weijun Wang, Tobias Weyand, Marco Andreetto, and Hartwig Adam. Mobilenets: Efficient convolutional neural networks for mobile vision applications, 2017. URL <https://arxiv.org/abs/1704.04861>.
- [10] Mostafa S. Ibrahim, Srikanth Muralidharan, Zhiwei Deng, Arash Vahdat, and Greg Mori. A hierarchical deep temporal model for group activity recognition. In *2016 IEEE Conference on Computer Vision and Pattern Recognition (CVPR)*, pages 1971–1980, June 2016. doi: 10.1109/CVPR.2016.217.
- [11] Simindokht Jahangard, Munawar Hayat, and Hamid Rezaatofghi. Real-time trajectory-based social group detection, 2023. URL <https://arxiv.org/abs/2304.05678>.
- [12] Simindokht Jahangard, Zhixi Cai, Shiki Wen, and Hamid Rezaatofghi. Jrd-db-social: A multifaceted robotic dataset for understanding of context and dynamics of human interactions within social groups. In *2024 IEEE/CVF Conference on Computer Vision and Pattern Recognition (CVPR)*, pages 22087–22097, June 2024. doi: 10.1109/CVPR52733.2024.02085.
- [13] Alex Krizhevsky, Ilya Sutskever, and Geoffrey E Hinton. Imagenet classification with deep convolutional neural networks. In F. Pereira, C.J. Burges, L. Bottou, and K.Q. Weinberger, editors, *Advances in Neural Information Processing Systems*, volume 25. Curran Associates, Inc., 2012. URL https://proceedings.neurips.cc/paper_files/paper/2012/file/c399862d3b9d6b76c8436e924a68c45b-Paper.pdf.
- [14] Tian Lan, Yang Wang, Weilong Yang, Stephen N. Robi-novitch, and Greg Mori. Discriminative latent models for recognizing contextual group activities. *IEEE Transactions on Pattern Analysis and Machine Intelligence*, 34(8):1549–1562, Aug 2012. ISSN 1939-3539. doi: 10.1109/TPAMI.2011.228.
- [15] Shuaicheng Li, Qianggang Cao, Lingbo Liu, Kunlin Yang, Shinan Liu, Jun Hou, and Shuai Yi. Group-former: Group activity recognition with clustered spatial-temporal transformer. In *2021 IEEE/CVF International Conference on Computer Vision (ICCV)*, pages 13648–13657, Oct 2021. doi: 10.1109/ICCV48922.2021.01341.
- [16] Zhengcen Li, Yueran Li, Linlin Tang, Tong Zhang, and Jingyong Su. Two-person graph convolutional network for skeleton-based human interaction recognition. *IEEE Trans. Cir. and Sys. for Video Technol.*, 33(7):3333–3342, July 2023. ISSN 1051-8215. doi: 10.1109/TCSVT.2022.3232373. URL <https://doi.org/10.1109/TCSVT.2022.3232373>.
- [17] Jun Liu, Amir Shahroudy, Mauricio Perez, Gang Wang, Ling-Yu Duan, and Alex C. Kot. Ntu rgb+d 120: A large-scale benchmark for 3d human activity understanding. *IEEE Transactions on Pattern Analysis and Machine Intelligence*, 42(10):2684–2701, Oct 2020. ISSN 1939-3539. doi: 10.1109/TPAMI.2019.2916873.
- [18] Ilya Loshchilov and Frank Hutter. Decoupled weight decay regularization, 2019. URL <https://arxiv.org/abs/1711.05101>.
- [19] Alonso Patron-Perez, Marcin Marszalek, Ian Reid, and Andrew Zisserman. Structured learning of human interactions in tv shows. *IEEE Transactions on Pattern Analysis and Machine Intelligence*, 34(12):2441–2453, Dec 2012. ISSN 1939-3539. doi: 10.1109/TPAMI.2012.24.
- [20] Mauricio Perez, Jun Liu, and Alex C. Kot. Interaction relational network for mutual action recognition. *IEEE Transactions on Multimedia*, 24:366–376, 2022. ISSN 1941-0077. doi: 10.1109/TMM.2021.3050642.
- [21] Mengshi Qi, Jie Qin, Annan Li, Yunhong Wang, Jiebo Luo, and Luc Van Gool. stag-net: An attentive semantic rnn for group activity recognition. In Vittorio Ferrari,

- Martial Hebert, Cristian Sminchisescu, and Yair Weiss, editors, *Computer Vision – ECCV 2018*, pages 104–120, Cham, 2018. Springer International Publishing. ISBN 978-3-030-01249-6.
- [22] M. S. Ryoo and J. K. Aggarwal. UT-Interaction Dataset, ICPR contest on Semantic Description of Human Activities (SDHA). http://cvrc.ece.utexas.edu/SDHA2010/Human_Interaction.html, 2010.
 - [23] Karen Simonyan and Andrew Zisserman. Very deep convolutional networks for large-scale image recognition, 2015. URL <https://arxiv.org/abs/1409.1556>.
 - [24] Mingxing Tan and Quoc V. Le. Efficientnet: Rethinking model scaling for convolutional neural networks, 2020. URL <https://arxiv.org/abs/1905.11946>.
 - [25] Angélique Taylor and Laurel D. Riek. Regroup: A robot-centric group detection and tracking system. In *2022 17th ACM/IEEE International Conference on Human-Robot Interaction (HRI)*, pages 412–421, March 2022. doi: 10.1109/HRI53351.2022.9889634.
 - [26] Xiaolong Wang, Ross Girshick, Abhinav Gupta, and Kaiming He. Non-local neural networks. In *2018 IEEE/CVF Conference on Computer Vision and Pattern Recognition*, pages 7794–7803, 2018. doi: 10.1109/CVPR.2018.00813.
 - [27] Yuxiao Wang, Yu Lei, Li Cui, Weiyang Xue, Qi Liu, and Zhenao Wei. A review of human-object interaction detection, 2025. URL <https://arxiv.org/abs/2408.10641>.
 - [28] Jianchao Wu, Limin Wang, Li Wang, Jie Guo, and Gangshan Wu. Learning actor relation graphs for group activity recognition. In *2019 IEEE/CVF Conference on Computer Vision and Pattern Recognition (CVPR)*, pages 9956–9966, June 2019. doi: 10.1109/CVPR.2019.01020.
 - [29] Hangjie Yuan, Dong Ni, and Mang Wang. Spatio-temporal dynamic inference network for group activity recognition. In *2021 IEEE/CVF International Conference on Computer Vision (ICCV)*, pages 7456–7465, Oct 2021. doi: 10.1109/ICCV48922.2021.00738.
 - [30] Hangjie Yuan, Dong Ni, and Mang Wang. Spatio-temporal dynamic inference network for group activity recognition. In *2021 IEEE/CVF International Conference on Computer Vision (ICCV)*, pages 7456–7465, Oct 2021. doi: 10.1109/ICCV48922.2021.00738.